



Interaction between nickel hydroxy phthalocyanine derivatives with p-chlorophenol: Linking electrochemistry experiments with theory

Samson Khene, Kevin Lobb, Tebello Nyokong*

Department of Chemistry, Rhodes University, Grahamstown 6140, South Africa

ARTICLE INFO

Article history:

Received 8 August 2010

Received in revised form

26 September 2010

Accepted 2 October 2010

Available online 25 October 2010

Keywords:

Nickel phthalocyanine

Chlorophenol

Hardness

Softness

Condensed Fukui function

ABSTRACT

In this work the interaction between peripherally (β) substituted nickel tetrahydroxyphthalocyanines (β -NiPc(OH)₄ and β -Ni(O)Pc(OH)₄) with p-chlorophenol is theoretically rationalised by performing calculations at B3LYP/6-31G(d) level. Density functional theory (DFT) and molecular orbital theory are used to calculate the condensed Fukui function for phthalocyanine derivatives and p-chlorophenol, in order to determine the reactive sites involved when p-chlorophenol is oxidized, and to compare theoretically predicted reactivity to experimentally determined electrocatalytic activity. Electrocatalytic activities of adsorbed NiPc derivatives: *ads*- α -NiPc(OH)₈-OPGE (OPGE = ordinary poly graphite electrode), *ads*- α -NiPc(OH)₄-OPGE and *ads*- β -NiPc(OH)₄-OPGE are compared with those of the polymerized counterparts: *poly*- α -Ni(O)Pc(OH)₈-OPGE, *poly*- α -NiPc(OH)₄-OPGE and *poly*- β -NiPc(OH)₄-OPGE, respectively.

© 2010 Elsevier Ltd. All rights reserved.

1. Introduction

Organic materials, such as phthalocyanines, have been used at electrode interface, in order to tune or improve the electron transfer properties of the electrode [1–4]. Density functional theory (DFT) methods have proved useful in elucidating chemical properties when molecules interact [5–8]. The DFT calculations are used in this paper to study chemical potential (μ), chemical hardness (η) and chemical softness (S) of nickel phthalocyanine tetrasubstituted with hydroxyl at the peripheral (β) positions (β -NiPc(OH)₄ and β -Ni(O)Pc(OH)₄, the latter was formed following transformed β -NiPc(OH)₄ in NaOH to form O–Ni–O bridges [9–11]) on interaction with p-chlorophenol. We also determine the reactive site by making use of the condensed Fukui function [6,12]. The Fukui function derived by Parr and Yang [6] is related to the electron density in the frontier molecular orbitals (FMO) and as a result it plays a crucial role in chemical selectivity [13]. In the previous work [14], the reactivity of β -NiPc(OH)₄ and β -Ni(O)Pc(OH)₄ towards the electrocatalysis of p-chlorophenol was determined using DFT methods.

The aim of this paper is to make use of the Fukui function in order to theoretically investigate if there will be any effect on selectivity and reactivity of the ring, due to the hydroxy group substituted at different positions on metallo phthalocya-

nines (Fig. 1). The Fukui function will give us information on possible reactive sites on the metallo phthalocyanine, where electrocatalytic oxidation of analytes such as 4-chlorophenol may occur. The Fukui function plots of three differently substituted metallo phthalocyanines {non-peripherally-(α -NiPc(OH)₄) and peripherally tetrasubstituted (β -NiPc(OH)₄) and non-peripherally octasubstituted (α -NiPc(OH)₈), Fig. 1} are comparatively studied and the information was used to explain their catalytic activity towards the oxidation of 4-chlorophenol. The electrocatalytic studies of these molecules towards the oxidation of 4-chlorophenol are also presented in this work. For the electrochemical studies the NiPc derivatives are adsorbed on ordinary poly graphite electrode (OPGE) to form *ads*- β -NiPc(OH)₄-OPGE, *ads*- α -NiPc(OH)₄-OPGE and *ads*- α -NiPc(OH)₈-OPGE or polymerized in NaOH to form, *poly*- β -Ni(O)Pc(OH)₄-OPGE, *poly*- α -Ni(O)Pc(OH)₄-OPGE and *poly*- α -Ni(O)Pc(OH)₈-OPGE, respectively. The latter contain O–Ni–O bridges as discussed above.

2. Theoretical background: interaction and reactivity descriptors

Chemical potential (μ), chemical hardness (η) and chemical softness (S) are three useful molecular indices in DFT framework. According to Koopman's theorem [15], the three quantities are defined by Eq. (1)–(3):

$$\mu = \left(\frac{\partial E}{\partial N} \right)_{v(r)} \approx \frac{1}{2}(\epsilon_{\text{HOMO}} + \epsilon_{\text{LUMO}}) \quad (1)$$

* Corresponding author. Tel.: +27 46 6038260; fax: +27 46 6225109.

E-mail address: t.nyokong@ru.ac.za (T. Nyokong).

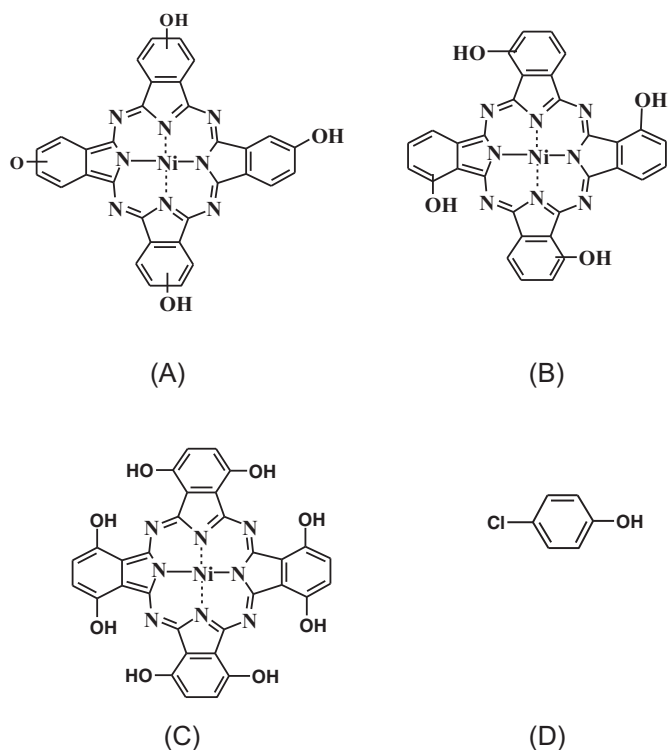


Fig. 1. Molecular structure of (A) β -NiPc(OH)₄, (B) α -NiPc(OH)₄, (C) α -NiPc(OH)₈, and (D) p-chlorophenol.

$$\eta = \frac{1}{2} \left(\frac{\partial \mu}{\partial N} \right)_{v(r)} = \frac{1}{2} \left(\frac{\partial^2 E}{\partial N^2} \right)_{v(r)} \approx \frac{1}{2} (\epsilon_{\text{LUMO}} - \epsilon_{\text{HOMO}}) \quad (2)$$

and

$$S = \left(\frac{\partial N}{\partial \mu} \right)_{v(r)} = \frac{1}{2\eta} \quad (3)$$

where E is energy of interacting molecules, $v(r)$ is the external electrostatic potential an electron at position (r) experiences due to the nuclei, N is the number of electrons, ϵ_{HOMO} is the energy of the highest occupied molecular orbital (HOMO) and ϵ_{LUMO} is the energy of the lowest unoccupied molecular orbital (LUMO). Chemical hardness (η) governs reactivity (Eq. (2)) [15,16]. When studying the chemical reactivity of two interacting molecules the chemical potential (μ) has an important role to play. In order for a reaction to proceed via a low-energy path, an electron should be transferred from a molecule with higher chemical potential to a molecule with a lower chemical potential [17]. This means that the larger the difference in the chemical potential between the two molecules, the easier the reaction will be.

If a reaction is to take place, the driving force in a reaction is the equalization of the chemical potential between the two reacting species. Changes in the number of electrons and the external potential will cause the chemical potential of a system to change. If only infinitesimal changes in μ are considered, the following relation is established, Eq. (4):

$$d\mu = \left(\frac{\partial^2 E}{\partial N^2} \right)_{v(r)} dN + \int \left(\frac{\delta \mu}{\delta v(r)} \right)_{N} \delta v(r) dr \quad (4)$$

The first term gives the chemical hardness shown in Eq. (2), which is an important factor governing the reactivity of two chemical species. The second term in Eq. (4) is related to the Fukui

function $f(r)$ which is defined by Eqs. (5) and (6):

$$f(r) = \left(\frac{\delta \mu}{\delta v(r)} \right)_{N} = \left(\frac{\partial \rho(r)}{\partial N} \right)_{v(r)} \quad (5)$$

$$\rho(r) = \left(\frac{\partial E}{\partial v(r)} \right)_{N} \quad (6)$$

where $\rho(r)$ is the electron density. In the DFT framework, the Fukui function is a local reactivity descriptor and provides the reactive site where the reaction occurs. The Fukui function gives the site of higher reactivity because the function gives the largest variation in the electronic density for a molecular system when it accepts or donates electrons.

The Fukui function (Eq. (5)) is a quantity involving the electron density of the atom or molecule in its frontier orbitals and has a local quantity which has different values at different points [18]. This function is indicative of how the electronic density varies at a constant external potential when there is a change in the number of electrons in the system. When electrons are added to the LUMO or removed from the HOMO, the density as a function of N has slope discontinuities, hence three different reaction indices can be defined, $f^+(r)$, $f^-(r)$ and $f^0(r)$ which are the Fukui functions for nucleophilic attack, electrophilic attack and radical attack, respectively. They are defined by Eqs. (7)–(9):

$$f^+(r) = \left(\frac{\partial \rho(r)}{\partial N^+} \right)_{v(r)} \approx \rho_{N+1}(r) - \rho_N(r) \quad (7)$$

$$f^-(r) = - \left(\frac{\partial \rho(r)}{\partial N^-} \right)_{v(r)} \approx \rho_N(r) - \rho_{N-1}(r) \quad (8)$$

$$f^0(r) = \left(\frac{\partial \rho(r)}{\partial N^0} \right)_{v(r)} \approx \frac{1}{2} [\rho_{N+1}(r) - \rho_{N-1}(r)] = \frac{1}{2} [f^+(r) + f^-(r)] \quad (9)$$

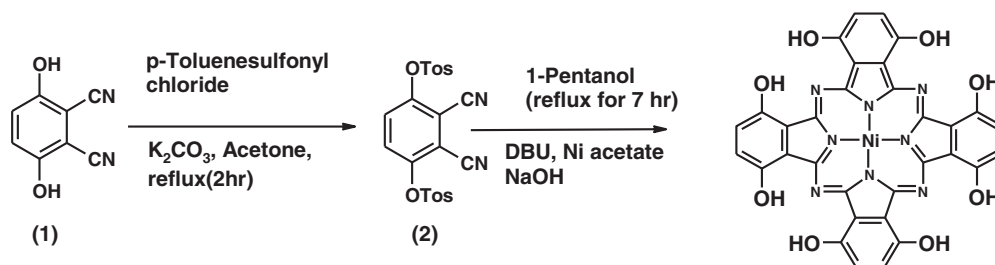
where $f^-(r)$, measures the reactivity towards an electrophile, $f^+(r)$, measures reactivity towards a nucleophile and $f^0(r)$ measures reactivity towards radical attack. The quantities $\rho_{N+1}(r)$, $\rho_N(r)$ and $\rho_{N-1}(r)$ are the electronic densities for the system with $N+1$, N and $N-1$ electrons, respectively.

When charges of two interacting molecules are small or may be zero, for example in a reaction between two neutral molecules, the maximal Fukui function ($f(r)$) site is preferred for the reaction [18]. When the charges of the molecules are relatively large, then the Fukui function ($f(r)$) needs to be minimised in order for the reaction to proceed smoothly [18,19].

3. Computational aspects and calculation procedure

In this work, Gaussian 03 program [20] running on an Intel/Linux cluster was used to perform all DFT calculations. The calculations were done at the B3LYP level with basis set 6-31G(d) for both optimization and excited energy calculations (using time dependent density function theory, TDDFT). Gausview 4.1 program was used for all visualization [20]. B3LYP employs Becke's method of using Lee–Yang–Parr's gradient-correction, exchange–correlation density functional, which includes a hybrid of the Hatree–Fock exchange and the DFT exchange.

Geometry optimization for the ground state of a given molecule A (e.g. β -NiPc(OH)₄) was obtained. From this calculation, the value of the energy for molecule A with N electrons ($E_A(N)$) and the Mulliken charges on the k th atom of the molecule ($q_{Ak}(N)$) were obtained. Single point energy calculations were performed on molecule A with $N-1$ and $N+1$ electrons. Accordingly $E_A(N-1)$,



Scheme 1. Synthesis pathway for non-peripherally substituted α -NiPc(OH)₈.

$q_{Ak}(N-1)$ and $E_A(N+1)$, $q_{Ak}(N+1)$ are obtained from the calculations.

Ionization potentials (IP_A) and electron affinities (EA_A) for molecule A, are calculated using Eqs. (10) and (11):

$$IP_A = E_A(N-1) - E_A(N) \quad (10)$$

$$EA_A = E_A(N+1) - E_A(N) \quad (11)$$

From the values obtained for A, absolute electronegativity, absolute hardness and absolute softness values, χ_A , η_A and S_A , respectively can be calculated using Eqs. (12)–(14):

$$\chi_A = \frac{1}{2}(IP_A + EA_A) \quad (12)$$

$$\eta_A = \frac{1}{2}(IP_A - EA_A) \quad (13)$$

$$S_A = \frac{1}{2\eta_A} \quad (14)$$

Mulliken charges for each of the k th atoms in A with N , $N-1$ and $N+1$ electrons, allow for the calculation of the condensed Fukui function according to Eqs. (15)–(17):

$$f_{Ak}^+ = q_{Ak}(N_A + 1) - q_{Ak}(N_A) \quad (15)$$

$$f_{Ak}^- = q_{Ak}(N_A) - q_{Ak}(N-1) \quad (16)$$

$$f_{Ak}^0 = \frac{1}{2}[q_{Ak}(N_A + 1) - q_{Ak}(N_A - 1)] = \frac{1}{2}[f_{Ak}^+ + f_{Ak}^-] \quad (17)$$

Condensed local softness is represented by Eqs. (18)–(20):

$$S_{Ak}^+ = S_A f_{Ak}^+ \quad (18)$$

$$S_{Ak}^- = S_A f_{Ak}^- \quad (19)$$

$$S_{Ak}^0 = S_A f_{Ak}^0 \quad (20)$$

4. Experimental

4.1. Materials

Nickel acetate tetrahydrate, diazabicyclo{5.4.0}-undec-7-ene (DBU), 1-pentanol, dimethylsulphoxide (DMSO), dicyano hydroquinone, sodium hydroxide, hydrochloric acid, sodium sulphide nonahydrate (Aldrich), sodium nitrite and p-toluenesulfonyl chloride were from Aldrich.

4.2. Synthesis of NiPc derivatives

The synthesis of peripherally substituted nickel hydroxyphthalocyanine (β -NiPc(OH)₄) has been reported in the literature [21]. The non-peripherally substituted derivative (α -NiPc(OH)₄) was synthesized and characterized as reported for the ZnPc derivative [22]. The synthesis of non-peripherally octahydroxy nickel phthalocyanine (α -NiPc(OH)₈) is briefly described as follows (see Scheme 1):

2,3-Dicyano-1,4-dihydroquinone (**1**) was converted to 3,6-bis(4-methylphenylsulfonyloxy) phthalonitrile (**2**) following the literature methods [23]. For the synthesis of α -NiPc(OH)₈, compound **2** (1 g, 2.13 mmol) and dry 1-pentanol (3 ml) were placed in a standard round bottom flask and refluxed for 30 min. Anhydrous nickel acetate tetrahydrate (0.13 g, 0.53 mmol) was added to the hot solution followed by a drop of DBU. The mixture was further refluxed for 7 h to afford α -NiPc(OTos)₈ (OTos = Tosyl). α -NiPc(OTos)₈ (0.77 g, 0.53 mmol) was stirred in NaOH (1 mol dm⁻³) solution for 24 h to afford α -NiPc(OH)₈. The product was separated and purified using 1 mol dm⁻³ sodium hydroxide, 1 mol dm⁻³ hydrochloric acid and finally with water. α -NiPc(OH)₈ was further stirred in hot methanol:water mixture (1:1) and finally dried at 80 °C overnight.

Yield 0.22 g (60%). ¹H NMR: δ_H (DMSO), 7.3–7.8 (8H, m, Ar-CH), 5.8 (Ar-OH); IR spectrum (cm⁻¹): 3314 (OH), 3057 (Ar-CH), 1588 (C=C), 1554 (C=N), 1491, 1474, 1361, 1286, 1172, 1142, 1081, 928, 812, 747, 704, 747. Calc. MS (ESI-MS) m/z : (NiPc(OH)₈) Calculated. 699; Found: 699 [M⁺].

A broad ¹H NMR singlet due to hydroxy substituent at 5.8 ppm, disappeared upon addition of D₂O.

4.3. Equipment

¹H NMR spectra were obtained, in deuterated solvents, using a Bruker EMX 400 MHz or Bruker Avance II+ 600 MHz NMR spectrometers. FT-IR spectra (KBr pellets) were recorded on a Perkin-Elmer spectrum 100 ATR spectrometer. MALDI-TOF mass spectra were recorded ABI Voyager DE-STR Maldi TOF instrument at University of Stellenbosch.

4.4. Electrochemical methods

Cyclic voltammograms (CV) were obtained using Autolab potentiostat PGSTAT 30 (Eco Chemie, Utrecht, The Netherlands) driven by the General Purpose Electrochemical Systems data processing software. A conventional three-electrode set up with ordinary poly graphite electrode (OPGE) as a working electrode, platinum wire as counter electrode and Ag|AgCl (3 M KCl) as a reference electrode was employed. The working electrode (OPGE) was constructed in house and the conduction between the copper wire and OPG material was facilitated by making use of high purity silver paint and Teflon was used for the outer casing. The OPGE (area = 0.44 cm²) was cleaned by polishing on 800 and 1200 grit emery paper, followed by rinsing with ultra-pure Millipore water.

The NiPc derivatives (β -NiPc(OH)₄, α -NiPc(OH)₄ and α -NiPc(OH)₈) were adsorbed onto the OPGE by dipping the electrode in dry dimethylsulfoxide (DMSO) containing NiPc derivative and allowing the solvent to dry to give adsorbed derivatives: ads - β -NiPc(OH)₄, ads - α -NiPc(OH)₄ and ads - α -NiPc(OH)₈, respectively. The electrochemical transformation of the NiPc derivatives in alkaline aqueous solution to form the interconnected O–Ni–O oxo bridges was achieved by cycling ads - β -NiPc(OH)₄, ads - α -NiPc(OH)₄ and ads - α -NiPc(OH)₈, in 0.1 mol dm⁻³ NaOH,

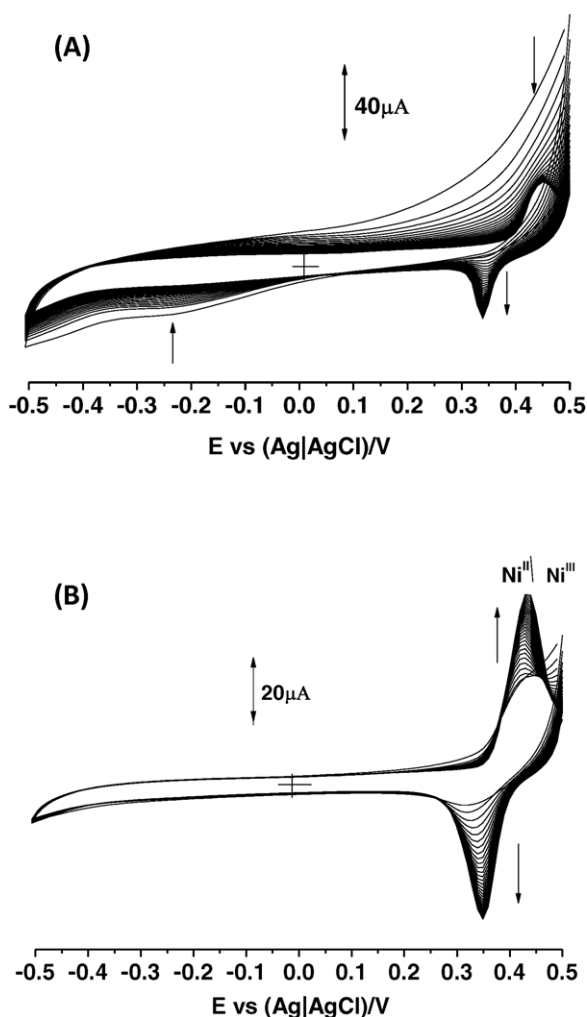


Fig. 2. Cyclic voltammograms of (A) *ads-α-NiPc(OH)₄*, and (B) *ads-α-NiPc(OH)₈* adsorbed on the OPG electrode in 0.1 mol dm⁻³ NaOH, forming *poly-α-Ni(O)Pc(OH)₄* and *poly-α-Ni(O)Pc(OH)₈*, respectively. Scan rate = 100 mV s⁻¹.

giving the polymerized derivatives: *poly-β-Ni(O)Pc(OH)₄*, *poly-α-Ni(O)Pc(OH)₄* and *poly-α-Ni(O)Pc(OH)₈*, respectively.

5. Results and discussion

5.1. Analysis of derivatives on OPGE

OPGE is made of ordered sheets of hexagonally bonded carbon atoms arranged in the same direction and has both basal and the edge planes. Pyrolytic graphite is anisotropic, very reproducible and slightly denser than natural graphite. It is more porous than glassy carbon, thus allows easy adsorption of electrode modifiers. Hence it was employed in this work.

Depositions of NiPc derivatives to form *ads-β-NiPc(OH)₄*, *ads-α-NiPc(OH)₄* and *ads-α-NiPc(OH)₈* on ordinary poly graphite electrode were performed by adsorption from 1 × 10⁻³ mol dm⁻³ solution of the complex in DMSO. The adsorption was performed by the dip dry method where the electrode was dipped in a solution of DMSO containing the NiPc derivative and then dried, resulting in adsorbed species. This was followed by recording of voltammograms in 0.1 mol dm⁻³ NaOH (Fig. 2). Fig. 2A shows only a weak feature at ~-0.2 V for *ads-α-NiPc(OH)₄*, this is due to the ring based reduction: (NiPc²⁻/NiPc³⁻) since adsorbed NiPc complexes do not show metal based (e.g. Ni^{III}Pc/Ni^{II}Pc or Ni^{II}Pc/Ni^IPc) processes. On cycling the adsorbed α-NiPc(OH)₄ in NaOH solution, Ni^{III}/Ni^{II} cou-

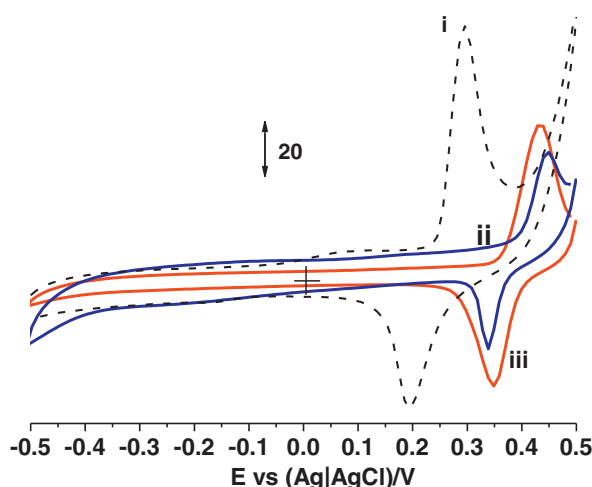


Fig. 3. Cyclic voltammograms of (i) *poly-β-Ni(O)Pc(OH)₄*, (ii) *poly-α-Ni(O)Pc(OH)₄* and (iii) *poly-α-Ni(O)Pc(OH)₈* on OPG electrode in 0.1 mol dm⁻³ NaOH. Scan rate = 100 mV s⁻¹.

ple began to form near 0.35 V. The cyclic voltammograms in Fig. 2A can be explained by the formation of the O–Ni–O oxo bridges in alkaline aqueous solution and are indication of the transformation of the NiPc(OH)₄ into the O–Ni–O oxo bridged to form *poly-α-Ni(O)Pc(OH)₄* [9–11]. Fig. 2B shows the cyclic voltammograms of *ads-α-NiPc(OH)₈* in 0.1 mol dm⁻³ NaOH. Unlike the case with *poly-α-Ni(O)Pc(OH)₄* (Fig. 2A) there was an immediate formation of a pair of peaks associated with Ni^{III}/Ni^{II} for *poly-α-Ni(O)Pc(OH)₈* (Fig. 2B). This was followed by a gradual increase of the current with scanning in 0.1 mol dm⁻³ NaOH. In the case of the reported *ads-β-NiPc(OH)₄* [14] the formation of Ni^{III}/Ni^{II} complexes was immediate compared to *ads-α-NiPc(OH)₄* where cycling was needed for formation of the couple as observed in Fig. 2A, showing that the ease of formation of O–Ni–O bridges depends on the point of substitution, with formation being easier for the peripherally substituted derivatives. Comparing the formation of *poly-α-Ni(O)Pc(OH)₄* with *poly-α-Ni(O)Pc(OH)₈*, the latter forms O–Ni–O bridges more readily than the former in that the peaks were formed instantly in the latter. Thus the ease of formation of the O–Ni–O bridges also depends on the number of substituents. The scan rate dependence of the peak current was linear, suggesting surface bound redox processes.

The type of substituent also plays a role. For example nickel tetrasulfophthalocyanine (NiTSPc) readily forms O–Ni–O oxo bridges without the need of activation, whereas for nickel tetraamino phthalocyanine (NiTAPc), activation is needed [9–11].

Fig. 3 overlays the cyclic voltammograms of (i) *poly-β-Ni(O)Pc(OH)₄*, (ii) *poly-α-Ni(O)Pc(OH)₄* and (iii) *poly-α-Ni(O)Pc(OH)₈* in 0.1 mol dm⁻³ NaOH. The peaks due to Ni^{III}/Ni^{II} are observed at $E_{1/2} = 0.39$ V for *poly-α-Ni(O)Pc(OH)₈*, 0.40 V for *poly-α-Ni(O)Pc(OH)₄* and at $E_{1/2} = 0.28$ V for *poly-β-Ni(O)Pc(OH)₄* in 0.1 mol dm⁻³ NaOH (Table 1). The Ni^{III}/Ni^{II} peaks for *poly-α-Ni(O)Pc(OH)₄* and *poly-α-Ni(O)Pc(OH)₈* occur at more positive potentials compared to *poly-β-Ni(O)Pc(OH)₄*, suggesting difficulty of oxidation for the former complexes which are non-peripherally substituted.

The surface coverage (Γ , mol cm⁻²) for *poly-β-Ni(O)Pc(OH)₄*, *poly-α-Ni(O)Pc(OH)₄* and *poly-α-Ni(O)Pc(OH)₈* was estimated from the charge under their relative oxidation peak using Eq. (21) [24]:

$$Q = nFA\Gamma \quad (21)$$

where Q is the total charge (C), A is the electrode surface area (0.07 cm²) and Γ is the surface coverage of the redox species.

Table 1
Electrochemical parameters for NiPc derivatives and 4-chlorophenol (7×10^{-4} mol dm $^{-3}$) electrocatalysis in 0.1 mol dm $^{-3}$ NaOH.

NiPc derivative	$E_{1/2}$ vs (Ag/AgCl)/V (NiIII/NiII) ^a	$10^{10} \times \Gamma^*$ (mol cm $^{-2}$) ^a	Number of NiPc derivative molecules ^{a,b}	EP vs (Ag/AgCl)/V (4-chlorophenol) ^c
<i>ads</i> - β -NiPc(OH) $_4$	–	–	–	0.26
<i>ads</i> - α -NiPc(OH) $_4$	–	–	–	– ^d
<i>ads</i> - α -NiPc(OH) $_8$	–	–	–	0.41
<i>poly</i> - β -Ni(O)Pc(OH) $_4$	0.28	1.49	6.0×10^{12} (2.9×10^{13})	0.39
<i>poly</i> - α -Ni(O)Pc(OH) $_4$	0.40	0.37	1.5×10^{12} (2.9×10^{13})	0.42, 0.45
<i>poly</i> - α -Ni(O)Pc(OH) $_8$	0.39	5.10	2.10×10^{13} (3.7×10^{10})	0.37

^a Values for adsorbed species were not determined due to Ni^{III}/Ni^{II} (or any clearly defined oxidation peak).

^b Numbers in brackets are theoretically calculated values.

^c The peak for oxidation on bare OPGE (ordinary poly graphite electrode) is 0.38 V.

^d No clearly defined peak.

Using Eq. (21), the total surface coverages of the electrodes of 5.10, 0.37, 1.49×10^{-10} mol cm $^{-2}$ were obtained for *poly*- α -Ni(O)Pc(OH) $_8$, *poly*- α -Ni(O)Pc(OH) $_4$ and *poly*- β -Ni(O)Pc(OH) $_4$ (Table 1).

The surface coverage values are within the order of magnitude of surface coverage expected for phthalocyanine molecule lying flat on the surface (10^{-10} mol cm $^{-2}$ [25]). *Poly*- α -Ni(O)Pc(OH) $_8$ gave a surface coverage larger than the monolayer value, while *poly*- α -Ni(O)Pc(OH) $_4$ gave a lower value. Only *poly*- β -Ni(O)Pc(OH) $_4$ gave a value near the monolayer. The differences reflect the ease of film formation for the NiPc derivatives. Number of molecules covering the surface area of the electrode was estimated experimentally using the surface coverage above and the geometric area of the OPGE, whereas the theoretical number of molecules (in brackets in Table 1) covering the surface area of the electrode were determined from optimized molecular structures (hence area of one molecule) using Gaussian at B3LYP/6-31G(d) level (Table 1). The calculated (theoretical) number of molecules for *poly*- α -Ni(O)Pc(OH) $_4$ and *poly*- β -Ni(O)Pc(OH) $_4$, are larger than the experimentally determined values, which suggest that the surface is less than a monolayer. For *poly*- α -Ni(O)Pc(OH) $_8$ the calculated number of molecules is much lower than the experimental values, which suggests that the surface coverage exceeds that of a monolayer.

5.2. Analysis of 4-chlorophenol

Please note that in this section the modified electrodes will be shown with OPGE at the end (as NiPc-OPGE) since the cyclic voltammetry on OPGE alone is also studied. Fig. 4A shows cyclic voltammograms of *ads*- β -NiPc(OH) $_4$ -OPGE (ii), and *poly*- β -Ni(O)Pc(OH) $_4$ -OPGE (iii) in the presence of p-chlorophenol. There is an increase in current for *poly*- β -Ni(O)Pc(OH) $_4$ -OPGE as compared to bare OPGE [14], showing catalytic activity. Catalytic activity is evidenced by enhancement of currents and lowering of potential compared to analysis on the unmodified electrode. The peak potential did not change for *poly*- β -Ni(O)Pc(OH) $_4$ but shifted to less positive values for *ads*- β -NiPc(OH) $_4$ -OPGE (Table 1), showing catalysis in terms of lowering of potential. The reduction of Ni(III) back to Ni(II) in Ni(O)Pc complexes is generally barely affected by the chlorophenols [11], but an enhancement in the Ni^{III} peak is observed when there is catalysis. In Fig. 4A, there is an increase in the anodic currents relative to the cathodic currents for *poly*- β -Ni(O)Pc(OH) $_4$ in the presence of 4-chlorophenol, hence confirming electrocatalysis. Plots of current (for p-chlorophenol) versus square root of scan rate (not shown) were linear for all the modified electrodes, confirming diffusion controlled mode of transport for p-chlorophenol.

Fig. 4B shows the cyclic voltammograms of 4-chlorophenol on bare (i), *ads*- α -NiPc(OH) $_4$ -OPGE (ii) and *poly*- α -Ni(O)Pc(OH) $_4$ -OPGE (iii). There is no peak observed for the oxidation 4-chlorophenol on *ads*- α -NiPc(OH) $_4$ -OPGE even though there is

one on bare OPGE. It is possible that the 4-chlorophenol peak occurs beyond the potential range of the OPGE. The peaks observed near -0.2 for *ads*- α -NiPc(OH) $_4$ -OPGE and near -0.3 for *poly*- α -Ni(O)Pc(OH) $_4$ -OPGE due to ring reduction (NiPc $^{2-}$ /NiPc $^{3-}$) process,

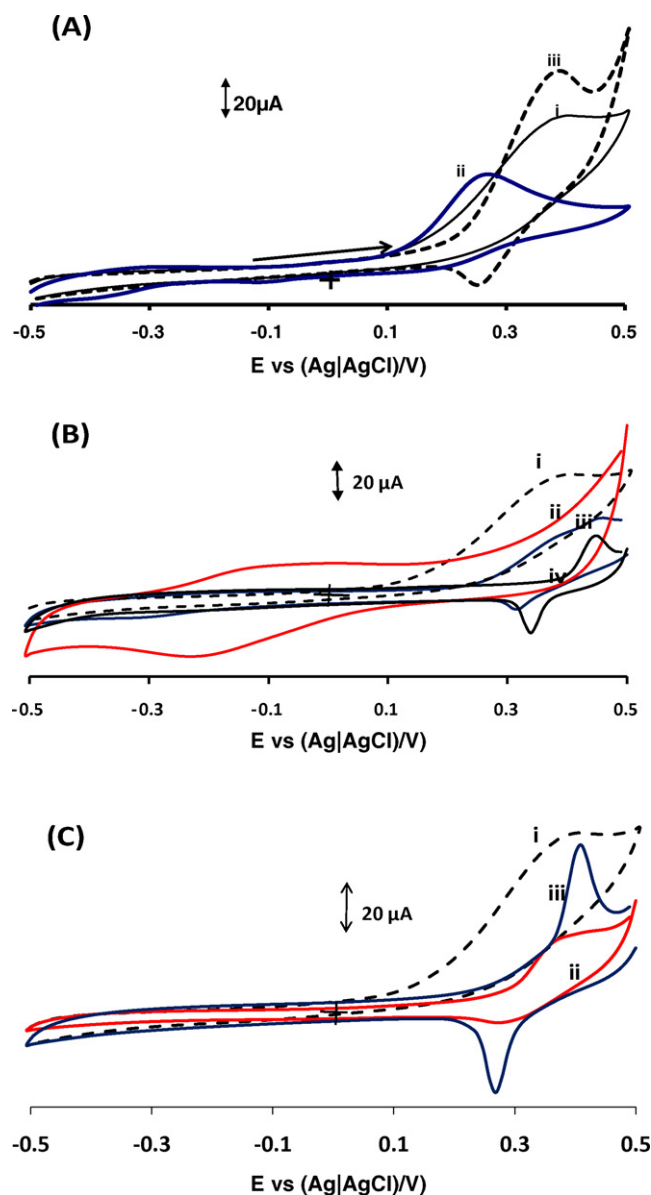


Fig. 4. Cyclic voltammograms of 7×10^{-4} mol dm $^{-3}$ 4-chlorophenol in 0.1 M NaOH on OPGE modified with (A) β -NiPc(OH) $_4$, (B) α -NiPc(OH) $_4$ and (C) α -NiPc(OH) $_8$. (i) Bare OPGE, (ii) adsorbed complexes and (iii) polymerized complexes containing O–Ni–O bridges. (iv) in (B) is for *poly*- α -Ni(O)Pc(OH) $_4$ on OPGE electrode in the absence of p-chlorophenol (in 0.1 mol dm $^{-3}$ NaOH). Scan rate = 100 mV s $^{-1}$.

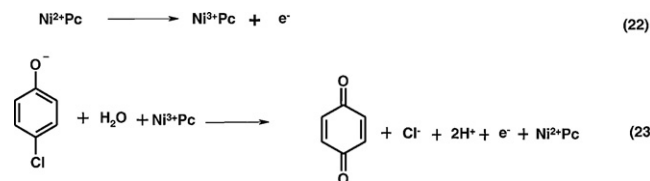
as discussed above (Fig. 2A). This process is not involved in the catalysis of 4-chlorophenol since it is at a much more negative potential than expected for the catalytic oxidation of this species. It has been reported that for the oxidation of 2-chlorophenol on poly NiTSPc (tetrasulfo phthalocyanine) two anodic peaks are observed [26]. The first appears at the same potential as for the bare electrode, followed by a second peak located at about 30 mV more positive than that of the potential of Ni^{III}/Ni^{II} couple in the absence of 2-chlorophenol but with higher currents. The two peaks are observed in Fig. 4B for the oxidation of 4-chlorophenol on (iii) *poly-α-Ni(O)Pc(OH)₄*-OPGE (Table 1). As stated above, the first peak for oxidation of 4-chlorophenol [26] appears at the same potential as for the bare electrode, followed by a second peak located at about 30 mV more positive than that of the potential of Ni^{III}/Ni^{II} couple in the absence of 2-chlorophenol but with higher currents. We suggest that first peak observed in Fig. 4B(iii) is due to oxidation of 4-chlorophenol on the part of the bare electrode not covered with and the second peak is due its oxidation on *poly-α-Ni(O)Pc(OH)₈*-OPGE.

Oxidation of 4-chlorophenol on *poly-α-Ni(O)Pc(OH)₄*-OPGE occurs with currents which are lower than those on bare OPGE, suggesting no catalytic activity compared to bare OPGE. However, there is an enhancement in the anodic currents of the Ni^{III}/Ni^{II} couple in the presence of 4-chlorophenol (Fig. 4B(iii)), compared with the cyclic voltammogram of *poly-α-Ni(O)Pc(OH)₄*-OPGE in the absence of 4-chlorophenol, suggesting the involvement of the former species in the oxidation process of the latter. However, since the currents for oxidation of 4-chlorophenol on bare OPGE are more than on *poly-α-Ni(O)Pc(OH)₄*-OPGE, catalytic activity cannot be proved convincingly.

Fig. 4C shows that the anodic current on bare OPGE (i) is higher than for *ads-α-NiPc(OH)₈*-OPGE(ii) and *poly-α-Ni(O)Pc(OH)₈*-OPGE (iii) modified electrodes for $7 \times 10^{-4} \text{ mol dm}^{-3}$ 4-chlorophenol. For the *ads-α-NiPc(OH)₈*-OPGE (ii), the currents for 4-chlorophenol are lower than for *poly-α-Ni(O)Pc(OH)₈*-OPGE (iii). Figs. 4C(iii) shows that the anodic currents for *poly-α-Ni(O)Pc(OH)₈*-OPGE in the presence of p-chlorophenol are higher than the cathodic currents confirming the involvement of the Ni^{III}/Ni^{II} couple in the oxidation of 4-chlorophenol.

In summary, for the oxidation of 4-chlorophenol on *poly-α-Ni(O)Pc(OH)₄*-OPGE and *poly-α-Ni(O)Pc(OH)₈*-OPGE, the observed currents are less than those of the bare OPGE, with no improvement in potential. However for *poly-β-Ni(O)Pc(OH)₄*-OPGE higher currents for 4-chlorophenol oxidation are observed than on bare OPGE showing good electrocatalytic activity compared to *poly-α-Ni(O)Pc(OH)₄*-OPGE and *poly-α-Ni(O)Pc(OH)₈*-OPGE. In terms of surface coverage, it would be expected that *poly-α-Ni(O)Pc(OH)₄*-OPGE ($\Gamma = 0.37 \times 10^{-10} \text{ mol cm}^{-2}$) would have lower catalytic currents than *poly-β-Ni(O)Pc(OH)₄*-OPGE ($\Gamma = 1.45 \times 10^{-10} \text{ mol cm}^{-2}$), as observed. *poly-α-Ni(O)Pc(OH)₈*-OPGE with the largest surface coverage ($\Gamma = 5.10 \times 10^{-10} \text{ mol cm}^{-2}$) would be expected to show better catalytic activity than the other two. This is not observed as discussed above since less currents are observed on *poly-α-Ni(O)Pc(OH)₄*-OPGE and *poly-α-Ni(O)Pc(OH)₈*-OPGE than on bare OPGE.

It can thus be concluded that non-peripheral substitution (α) does not favour electrocatalytic oxidation of 4-chlorophenols. The behaviour could be related to the ease of formation and nature of the O–Ni–O bridges, which form more readily for *poly-β-Ni(O)Pc(OH)₄* compared to either *poly-α-Ni(O)Pc(OH)₄* or *poly-α-Ni(O)Pc(OH)₈*. The better catalysis observed for *poly-β-Ni(O)Pc(OH)₄* could also be due to the fact the Ni^{III}/Ni^{II} peaks are observed at a much lower potential (0.28 V) when compared to *poly-α-Ni(O)Pc(OH)₄*-OPGE and *poly-α-Ni(O)Pc(OH)₈*-OPGE (0.40 and 0.39 V, respectively) (Table 1).



Scheme 2. Proposed mechanism for the catalytic oxidation of 4-chlorophenols by *poly-β-Ni(O)Pc(OH)₄* derivatives.

The mechanism for the oxidation of 4-chlorophenol in basic media may be proposed as shown by Scheme 2, Eqs. (22) and (23) [27] on *poly-β-Ni(O)Pc(OH)₄* where clear catalytic activity was involved:

In highly basic media (such as 0.1 mol dm^{-3} NaOH), 4-chlorophenol is deprotonated. The first step is the electrochemical oxidation of Ni^{II} to Ni^{III} for *poly-β-Ni(O)Pc* (Eq. (22)), followed by the reaction of Ni^{III} with deprotonated 4-chlorophenol in the presence of water molecules from electrolyte to form benzoquinone (Eq. (23)). Quinones are well known as products of electrocatalytic oxidation of chlorophenols [10]. For the adsorbed species, it is possible that ring based processes of the NiPc derivatives are involved since Ni^{III}/Ni^{II} are not known when NiPc derivatives are not polymerized.

5.3. Theoretical results

Molecular orbital calculations together with Fukui functions, hardness and softness indices, were used to analyse the chemical interaction of $\beta\text{-NiPc(OH)₄}$ and $\beta\text{-Ni(O)Pc(OH)₄}$ with p-chlorophenol.

In this paper the interaction between $\beta\text{-NiPc(OH)₄}$ and p-chlorophenol and the effect of the central metal is studied further than reported in Ref. [14], by making use of the condensed Fukui function (f_{Ak}^+), in order to increase our understanding of the electron transfer process. The theoretical calculations are compared with experimental results.

Fig. 5A shows optimized structure of $\beta\text{-NiPc(OH)₄}$ and p-chlorophenol adduct. The energy levels of $\beta\text{-H}_2\text{Pc(OH)₄}$, $\beta\text{-NiPc(OH)₄}$ and $\beta\text{-Ni(O)Pc(OH)₄}$ and the interaction of the latter two with 4-chlorophenol were calculated (Table 2). The HOMO–LUMO energy gaps of $\beta\text{-H}_2\text{Pc(OH)₄}$, $\beta\text{-NiPc(OH)₄}$ and $\beta\text{-Ni(O)Pc(OH)₄}$ HOMO–LUMO gap are 2.11 eV, 2.19 eV and 2.06 eV, respectively (Table 2).

We previously used the donor acceptor molecular hardness (η_{DA}) factor to study the interaction of p-chlorophenol and the NiPc complexes [14], the result obtained suggested that the $\beta\text{-Ni(O)Pc(OH)₄}$ ($\eta_{\text{DA}} = 1.87 \text{ eV}$) interacted better with p-chlorophenol compared to $\beta\text{-NiPc(OH)₄}$ ($\eta_{\text{DA}} = 1.98 \text{ eV}$). In this work, we used a more explicit and quantitative description of the interaction energy between the NiPc complexes and p-chlorophenol which agreed much better with experimental data. The intermolecular interaction energy calculations were obtained using the supramolecular

Table 2
Calculated HOMO–LUMO energy gaps (eV) in gas phase. References in parentheses.

Molecules	HOMO–LUMO (eV)
$\beta\text{-H}_2\text{Pc(OH)4}$	2.11
$\beta\text{-NiPc(OH)4}$	2.19 [14]
$\beta\text{-Ni(O)Pc(OH)4}$	2.06 [14]
$\beta\text{-NiPc(OH)4}/\text{p-chlorophenol}$	2.17
$\text{Ni(O)Pc(OH)4}/\text{p-chlorophenol}$	1.64
p-Chlorophenol	6.01

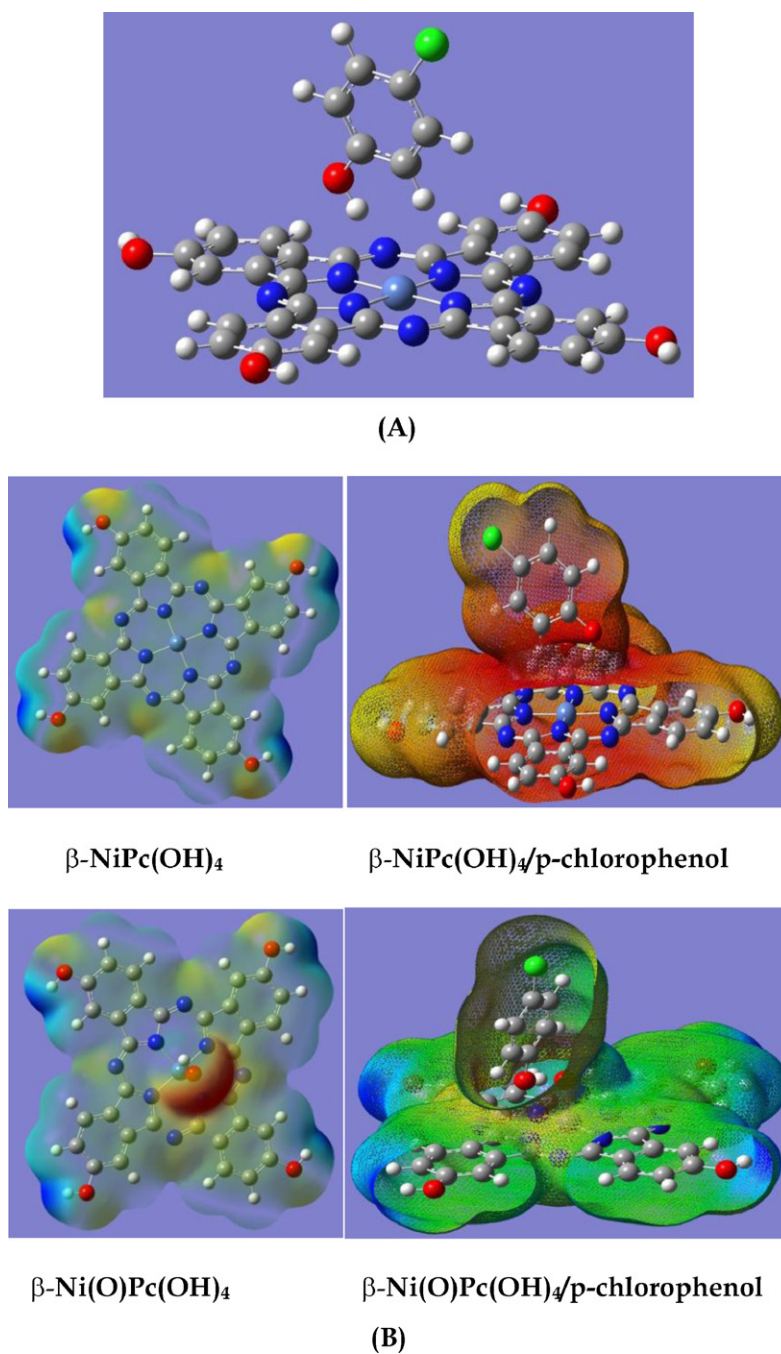


Fig. 5. (A) Optimized structure of $\beta\text{-NiPc(OH)}_4$ and p-chlorophenol using B3LYP/6-3g(d). (B) Electron density distribution of $\beta\text{-NiPc(OH)}_4$ in the absence and presence of and p-chlorophenol $\beta\text{-Ni(O)Pc(OH)}_4$ in the absence and presence of p-chlorophenol.

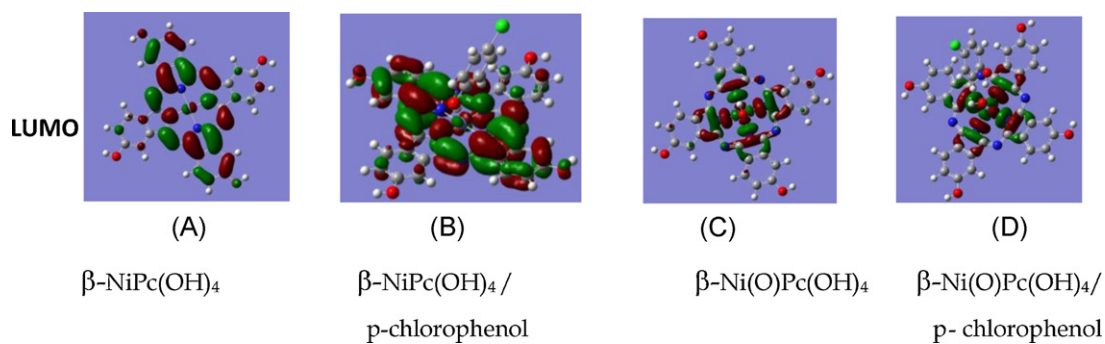


Fig. 6. $\beta\text{-NiPc(OH)}_4$ (A), $\beta\text{-NiPc(OH)}_4/\text{p-chlorophenol}$ (B), $\beta\text{-Ni(O)Pc(OH)}_4/\text{p-chlorophenol}$ (C) and $\beta\text{-Ni(O)Pc(OH)}_4$ (D) frontier molecular orbitals (LUMO).

approach, using Eq. (24):

$$E_{\text{int}} = E_{\text{complex}} - \sum E_{\text{molecules}} \quad (24)$$

where E_{int} is the interaction energy of the molecules, E_{complex} is the energy of the complex (NiPc/p-chlorophenol) and $\sum E_{\text{molecules}}$

is the sum total energy of isolated NiPc and p-chlorophenol. Interaction energy of p-chlorophenol and NiPc complexes was calculated using DFT calculations to be -205.9 kcal/mol ($\beta\text{-NiPc(OH)}_4$) and 19.1 kcal/mol ($\beta\text{-Ni(O)Pc(OH)}_4$). Fig. 5B shows the electron density distribution before and after the formation of the adduct. The interaction energy suggests that there

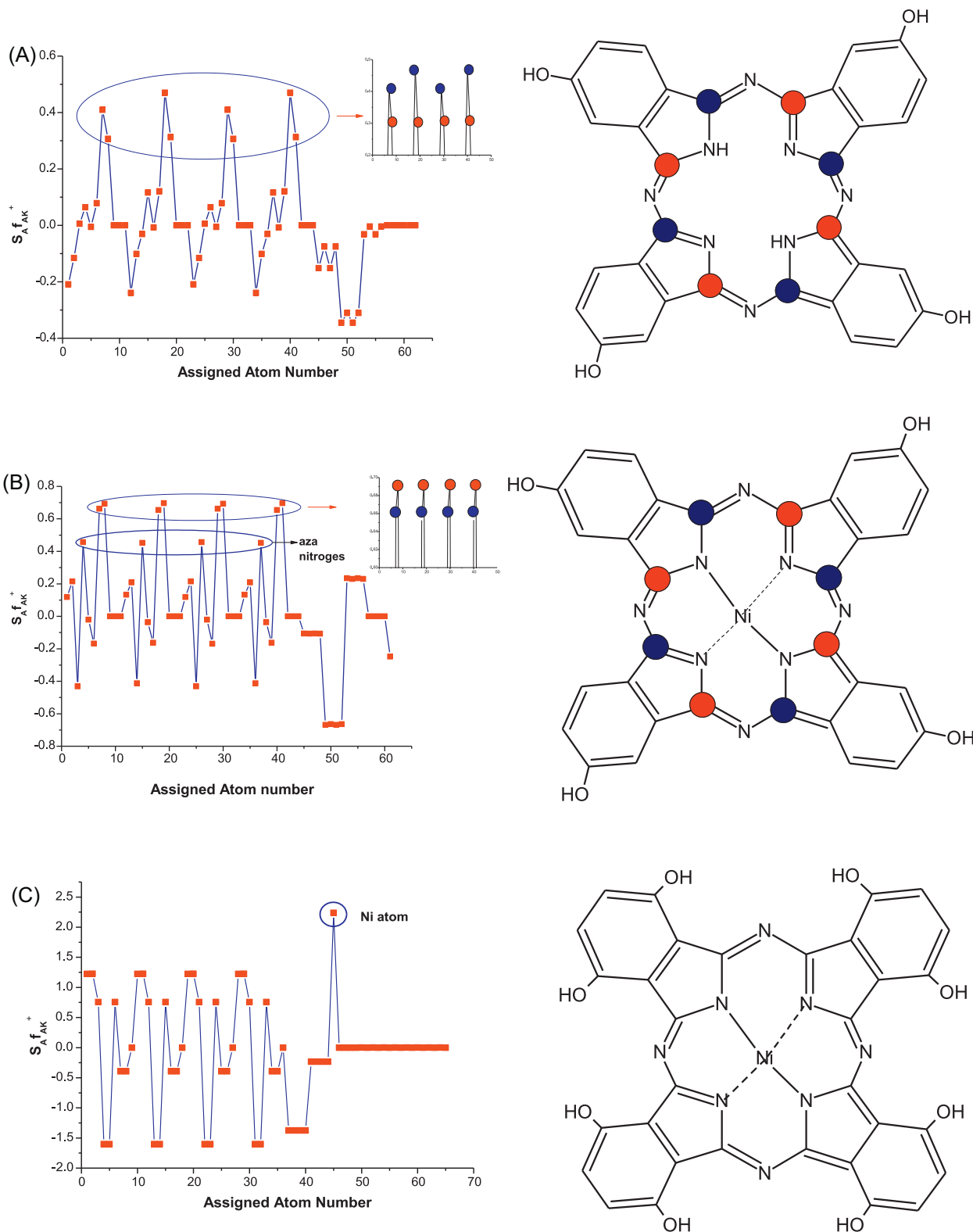


Fig. 7. Fukui 2D plots of condensed softness for maximum softness, $H_2Pc(OH)_4$ (A), $\beta\text{-NiPc(OH)}_4$ (B), $\alpha\text{-NiPc(OH)}_8$ (C), NiPc (D), and $\alpha\text{-NiPc(OH)}_4$ (E). (F) Atomic numbering in the phthalocyanine molecule which is used for describing peripheral and non-peripheral positions.

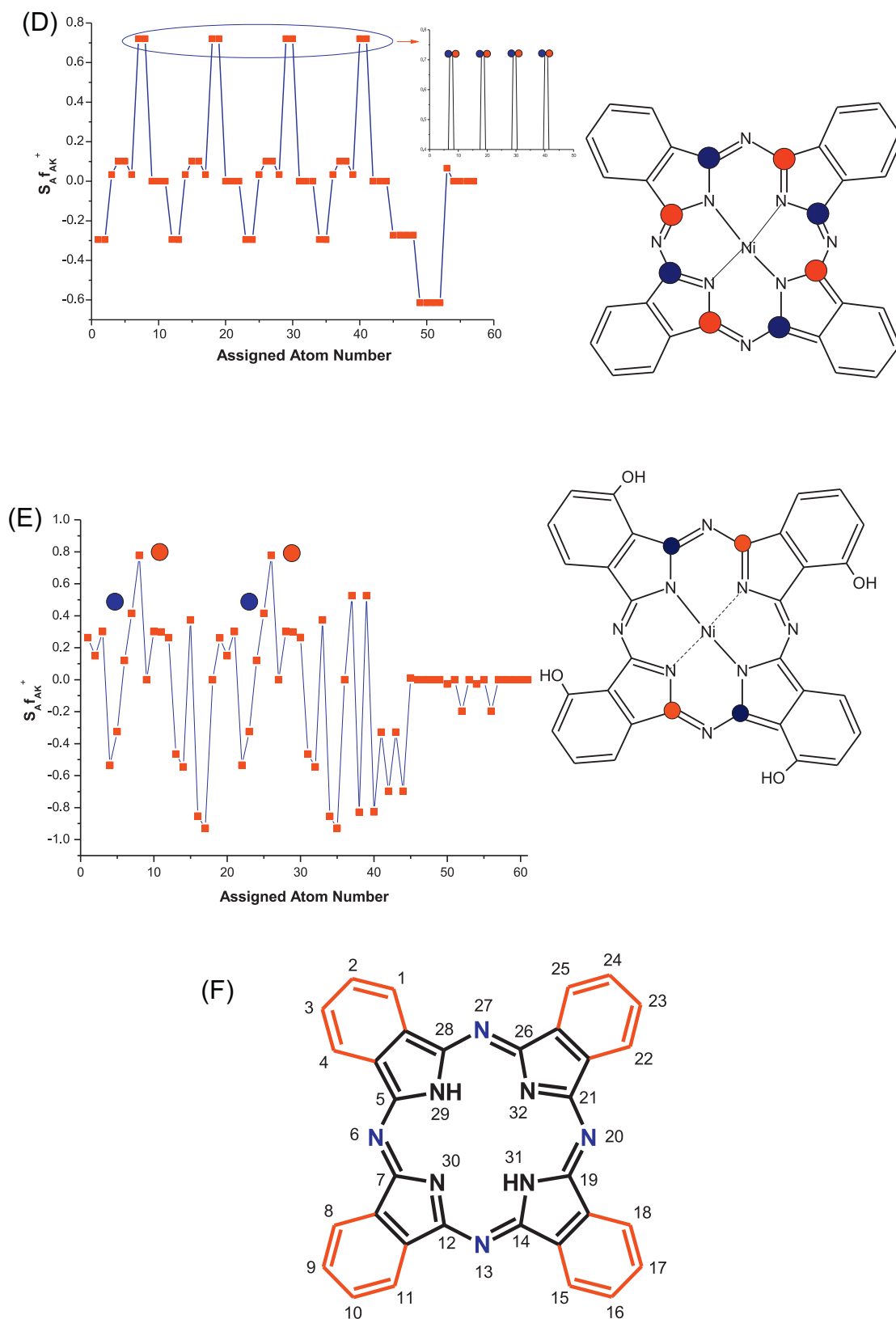


Fig. 7. (Continued).

is greater interaction of *p*-chlorophenol with β -NiPc(OH)₄ than with β -Ni(O)Pc(OH)₄. This is evidenced by shifting of the oxidative peak towards less positive potentials for β -NiPc(OH)₄ (Fig. 4A) compared to β -Ni(O)Pc(OH)₄ in the presence of chlorophenol.

The opposite was observed when we employed η_{DA} values [14]. The results suggest that one has to be very careful when using molecular indices to study interaction between supramolecular complexes.

Fig. 6A shows that for β -NiPc(OH)₄ the frontier MO (LUMO) is localized on the ligand and partly on the Ni atom. Also Fig. 6 shows that the LUMO of β -NiPc(OH)₄ appear as an antibonding pi orbital (π^*) and the LUMO of β -Ni(O)Pc(OH)₄ appear as an antibonding sigma orbital (σ^*). When β -NiPc(OH)₄ interacts with p-chlorophenol (Fig. 6B) the LUMO shows extensive localization of MO mainly on the Pc ligand with some on the Ni atom. For β -Ni(O)Pc(OH)₄ in the presence p-chlorophenol (Fig. 6D), there is less extensive delocalization on the Pc ring compared to when β -NiPc(OH)₄ interacts with p-chlorophenol. This suggests that for β -NiPc(OH)₄ the ring is more extensively involved in the oxidation of 4-chlorophenol when compared to β -Ni(O)Pc(OH)₄. When adsorbed specie (without cycling or conditioning in 0.1 mol dm⁻³ NaOH) are employed for the catalytic oxidation of 4-chlorophenol, the oxidation potentials are observed at different values compared to when the electrode has been cycled in 0.1 mol dm⁻³, suggesting that there are different catalytic sites involved. Following cycling in 0.1 mol dm⁻³, there will be sites containing Ni^{III}/Ni^{II}, hence the central metal will be involved in the catalytic reaction.

The oxidation process of p-chlorophenol is viewed as a nucleophilic attack of β -NiPc(OH)₄ by p-chlorophenol. According to Eqs. (7)–(9) and (15)–(17), in order to calculate the Fukui function and condensed Fukui function ($f(r)$ and f_{Ak}^+), one needs to determine the electron density of the molecule and the charges of the atoms in the molecule. In this work we have used the Mulliken gross population analysis for q_{Ak} , Eqs. (15) and (18) to determine the condensed Fukui function and the condensed local softness.

Tetra substituted phthalocyanine derivatives contain a mixture of four possible structural isomers, with the position of the substituents being at 2(3), 9(10), 16(17) and 23(24) for the peripherally substituted derivatives and at 1(4), 6(11), 15(18) and 22(25) for non-peripherally substituted derivatives (see numbering in Fig. 7). However for the purposes of the present calculations, the substituents have been fixed to one position on each benzene group. Fig. 7A–E gives us a clearer picture of what is actually happening to the carbons attached to nitrogens when H₂Pc(OH)₄ is metallated. Comparing Fig. 7A and B, we see that the condensed local softness (less reactive) values for carbons at 5, 12, 19, 26 (red region) lie below the ones at 7, 14, 21, 28 (blue regions), for unmetallated H₂Pc(OH)₄ (Fig. 7A). Upon metallation (Fig. 7B) the condensed local softness values for carbons at 5, 12, 19, 26 (red region) have increased (more reactive) to a point where they have surpassed the values for carbons at 7, 14, 21, 28 (blue regions).

Fig. 7A and B suggests that when Ni is inserted into the ring, the carbon atoms at 5, 12, 19, 26 (red region) are activated differently compared to unmetallated. The 5, 12, 19, 26 (red region) carbons are situated on the side where the OH is substituted and show greater local softness (hence greater reactivity). The carbons at 7, 14, 21, 28 (blue regions) are situated on the side where there are no OH substituents and have lower local softness values (less reactive compared to 5, 12, 19, 26 carbons). This suggests that even though the OH substituents have no effect on the bond length between the Ni atom and the N [14], it has some destabilization effect on the 5, 12, 19, 26 carbons for β -NiPc(OH)₄. Fig. 7D shows that for unsubstituted NiPc all the carbons are activated equally compared to β -NiPc(OH)₄. Fig. 7C suggests that, for α -NiPc(OH)₈, the Ni atom is made softer or more reactive relative to all other atoms. The Fukui plots of α -NiPc(OH)₈ suggests that if this complex was to be used for electro catalytic oxidation of p-chlorophenol, catalysis through the nickel atom would be favoured over the ring. Fig. 7E shows the Fukui plots of α -NiPc(OH)₄, showing that only the carbons are activated. It is observed experimentally that α -NiPc(OH)₄ and α -NiPc(OH)₈ shows bad catalytic activity towards the oxidation of

4-chlorophenol compared to β -NiPc(OH)₄ in terms of catalytic currents (Fig. 4).

6. Conclusions

NiPc derivatives: *poly- α -Ni(O)Pc(OH)₄-OPGE*, *poly- α -Ni(O)Pc(OH)₈-OPGE* and *poly- β -Ni(O)Pc(OH)₄-OPGE* and their adsorbed counterparts (*ads- α -NiPc(OH)₄-OPGE*, *ads- α -NiPc(OH)₈-OPGE* and *ads- β -NiPc(OH)₄-OPGE*) were studied for their catalytic activity towards the oxidation of p-chlorophenol. In terms of electrocatalytic activity, *poly- α -Ni(O)Pc(OH)₄-OPGE* and *poly- α -Ni(O)Pc(OH)₈-OPGE*, showed evidence for the involvement of the Ni^{III}/Ni^{II} couple in the oxidation of 4-chlorophenol, but the catalytic currents were less than those of the bare OPGE. *Poly- β -Ni(O)Pc(OH)₄-OPGE* showed higher currents than the bare OPGE showing good electrocatalytic activity compared to for *poly- α -Ni(O)Pc(OH)₄-OPGE* and *poly- α -Ni(O)Pc(OH)₈-OPGE*. We have shown, using interaction energy values that when p-chlorophenol interacts better with β -NiPc(OH)₄ than β -Ni(O)Pc(OH)₄, hence the former is a better catalyst in terms of lowering of overpotential. We have used the condensed Fukui function to determine the reactive sites where electron transfer would take place between p-chlorophenol and the nickel phthalocyanine complexes. We have theoretically rationalised the interaction of p-chlorophenol with nickel phthalocyanine complexes.

Acknowledgements

This work was supported by the Department of Science and Technology (DST) and National Research Foundation (NRF) of South Africa through DST/NRF South African Research Chairs initiative for Professor of Medicinal Chemistry and Nanotechnology and Rhodes University.

References

- [1] T. Nyokong, in: J.H. Zagal, F. Bedioui, J.-P. Dodelet (Eds.), *N4-Macrocyclic Metal Complexes*, Springer, United States of America, 2006.
- [2] D.R. Trackley, G. Dent, W.E. Smith, *Phys. Chem. Chem. Phys.* 2 (2001) 1419.
- [3] M.S. Ureta-Zanartu, P. Bustos, C. Berrios, M.C. Diez, M.L. Mora, C. Gutierrez, *Electrochim. Acta* 47 (2002) 2399.
- [4] S. Griveau, F. Bedioui, *Electroanalysis* 13 (2001) 253.
- [5] G. Heimel, L. Romaner, J.-L. Bredas, E. Zojer, *Phys. Rev. Lett.* 96 (2006) 196806.
- [6] R.G. Parr, W. Yang, *J. Am. Chem. Soc.* 106 (1984) 4049.
- [7] R.G. Parr, R.A. Donnelly, M. Levy, W.E. Palke, *J. Chem. Phys.* 68 (1978) 3801.
- [8] R.G. Parr, R.G. Pearson, *J. Am. Chem. Soc.* 105 (1983) 7512.
- [9] M.S. Ureta-Zanartu, A. Alarcon, C. Berrios, G.I. Cardenas-Jiron, J. Zagal, C. Gutierrez, *J. Electroanal. Chem.* 580 (2005) 94.
- [10] M.S. Ureta-Zañartu, C. Berrios, J. Pavez, J. Zagal, C. Gutierrez, J.F. Marco, *J. Electroanal. Chem.* 553 (2003) 147.
- [11] C. Berrios, M.S. Ureta-Zañartu, C. Gutierrez, *Electrochim. Acta* 53 (2007) 792.
- [12] P.W. Ayres, R.G. Parr, *J. Am. Chem. Soc.* 122 (2000) 2010.
- [13] M. Berkowitz, *J. Am. Chem. Soc.* 109 (1987) 4823.
- [14] S. Khene, K. Lobb, T. Nyokong, *Inorg. Chim. Acta* 362 (2009) 5055.
- [15] R.G. Pearson, *Acc. Chem. Res.* 26 (1993) 250.
- [16] B.E. Douglas, D.H. McDaniels, J.J. Alexander, *Concept and Models of Inorganic Chemistry*, John Wiley and Sons, Inc., New York, 1994, pp. 193–195.
- [17] Y. Li, J.N.S. Evans, *J. Am. Chem. Soc.* 117 (1995) 7756.
- [18] F. Mendez, J.L. Gazquez, *J. Am. Chem. Soc.* 116 (1994) 9298.
- [19] K. Flurchick, L. Bartolotti, *J. Mol. Graph.* 13 (1995) 10.
- [20] M.J. Frisch, G.W. Trucks, H.B. Schlegel, G.E. Scuseria, M.A. Robb, J.R. Cheeseman, J.A. Montgomery Jr., T. Vreven, K.N. Kudin, J.C. Burant, J.M. Millam, S.S. Iyengar, J. Tomasi, V. Barone, B. Mennucci, M. Cossi, G. Scalmani, N. Rega, G.A. Petersson, H. Nakatsuji, M. Hada, M. Ehara, K. Toyota, R. Fukuda, J. Hasegawa, M. Ishida, T. Nakajima, Y. Honda, O. Kitao, H. Nakai, M. Klene, X. Li, J.E. Knox, H.P. Hratchian, J.B. Cross, V. Bakken, C. Adamo, J. Jaramillo, R. Gomperts, R.E. Stratmann, O. Yazyev, A.J. Austin, R. Cammi, C. Pomelli, J.W. Ochterski, P.Y. Ayala, K. Morokuma, G.A. Voth, P. Salvador, J.J. Dannenberg, V.G. Zakrzewski, S. Dapprich, A.D. Daniels, M.C. Strain, O. Farkas, D.K. Malick, A.D. Rabuck, K. Raghavachari, J.B. Foresman, J.V. Ortiz, Q. Cui, A.G. Baboul, S. Clifford, J. Cioslowski, B.B. Stefanov, G. Liu, A. Liashenko, P. Piskorz, I. Komaromi, R.L. Martin, D.J. Fox, T. Keith, M.A. Al-Laham, C.Y. Peng, A. Nanayakkara, M. Challacombe, P.M.W. Gill, B. Johnson, W. Chen, M.W. Wong, C. Gonzalez, J.A. Pople, *Gaussian 03, Revision E.01*, Gaussian, Inc., Wallingford, CT, 2004.
- [21] B.N. Achar, P.K. Jayasree, *Synth. Met.* 104 (1999) 101.

- [22] C.C. Leznoff, M. Hu, C.R. McArthur, Y. Qin, J.E. van Lier, *Can. J. Chem.* 72 (1994) 1990.
- [23] S. Khene, D.A. Geralo, C.A. Togo, J. Limson, T. Nyokong, *Electrochim. Acta* 54 (2008) 183.
- [24] H.O. Finklea, in: A.J. Bard, I. Rubinstein (Eds.), *Electroanalytical Chemistry*, vol. 19, Marcel Dekker, New York, 1996, pp. 109–335.
- [25] Z. Li, M. Lieberman, W. Hill, *Langmuir* 17 (2001) 4887.
- [26] C. Berrius, J.F. Marco, C. Gutierrez, M.S. Ureta-Zañartu, *Electrochim. Acta* 54 (2009) 6425.
- [27] B. Agboola, T. Nyokong, *Electrochim. Acta* 52 (2007) 5039.